PROCEEDINGS OF SCIENCE

Precision measurement of the fluxes of electrons and positrons in Primary Cosmic Rays up to the TeV with the Alpha Magnetic Spectrometer

Matteo Duranti*
Università degli Studi and INFN Sez. Perugia, 06100 Perugia, Italy
E-mail: matteo.duranti@pg.infn.it
on behalf of the AMS Collaboration

The AMS-02 detector is operating on the International Space Station (ISS) since May 2011. More than 65 billion events have been collected by the instrument in the first four years of data taking. The analysis of the data collected by the instrument in the first 30 months led to the measurement of the positron fraction [2] and of the fluxes of electrons (e^-), positrons (e^+) [3] and electron plus positrons ($e^+ + e^-$) [4]. In this contribution we will review the analysis techniques used in the flux measurements and in particular for the combined electron plus positron energy spectrum measurement.

The 34th International Cosmic Ray Conference,
30 July- 6 August, 2015
The Hague, The Netherlands

*Speaker.

PoS(ICRC2015)273

1. Introduction

The Alpha Magnetic Spectrometer, AMS-02, is a general purpose high energy particle physics detector. It was launched into space with the Space Shuttle STS-134 mission and installed onboard the ISS in 2011, on May 19*th*, to conduct a unique long duration mission (up to the lifetime of the ISS) of fundamental physics research in space. The experimental challenge of this experiment is the accurate measurement of the Cosmic Rays (CR) composition and energy spectra, up to the TeV scale, that could reveal the presence of primordial anti-matter or give the signature of exotic sources, as for example secondaries from dark matter annihilation. In this contribution we will focus our discussion on the AMS-02 precision measurement of the fluxes of Cosmic Ray electrons and positrons: positrons in the energy range 0.5-500 GeV based on the analysis of 0.58 million e^+, electrons in the energy range 0.5-700 GeV based on 9.23 million e^- and electron plus positron in the energy range 0.5-1000 GeV based on 10.6 million $e^+ + e^-$. The analyzed electrons and positrons have been selected in the first 30 months of operations.
CR electrons and positrons (CRE) represent only a small fraction of the CR reaching the Earth's atmosphere; nevertheless the relevance of the measurement of their energy spectra and charge composition is fully recognized and has triggered a continuous experimental effort during the last 50 years.
Due to their light masses, the energy losses experienced by the CRE during their propagation in the Galaxy are fundamentally different with respect to those of the nuclear components; moreover, the features of the CRE energy spectrum above $\sim$ 10 GeV are sensitive to the production in nearby sources [19]. An excess of $e^+ + e^-$ in the range 300-700 GeV with respect to the expected from conventional diffuse electron sources has been reported by ATIC [5] and PPB-BETS [6]. The subsequent measurements of FERMI [7, 8] observed a spectral flattening of the CR $e^+ + e^-$ spectrum between 70-200 GeV and a milder excess of the CR $e^+ + e^-$ at higher energies with respect to ATIC and PPB-BETS. At higher energies, a rapid steepening of the spectrum is observed by HESS [18, 17]. The PAMELA measurements of the positron fraction [9] and of the electron spectrum [20] have pointed to the need of a *fresh* source of electrons and positrons contributing to the observed features in the high energy part of the CRE spectra. Accurate measurements of the features of the CRE up to the TeV energies can shed light on the origin of such observed features, either due to exotic sources as dark matter particles or due to other astrophysical sources such as pulsars [10, 11, 12, 13]. This motivated the high statistics, low systematics, long term AMS-02 campaign of data taking.

2. The AMS-02 Detector

The layout of the AMS-02 detector [1] is shown in Fig.1 (left). The event display of a 660 GeV electron (e^-) reported in Fig.1 (right) shows how the particle identification is achieved by means of the different subsystems. The Time Of Flight (TOF) system defines the arrival direction of the particle as downward-going in the apparatus and measures its unitary charge and velocity. Nine layers of double sided silicon microstrip detectors, the Silicon Tracker, are used to reconstruct the particle trajectory in the 0.14 T magnetic field of the permanent magnet. The particle momentum

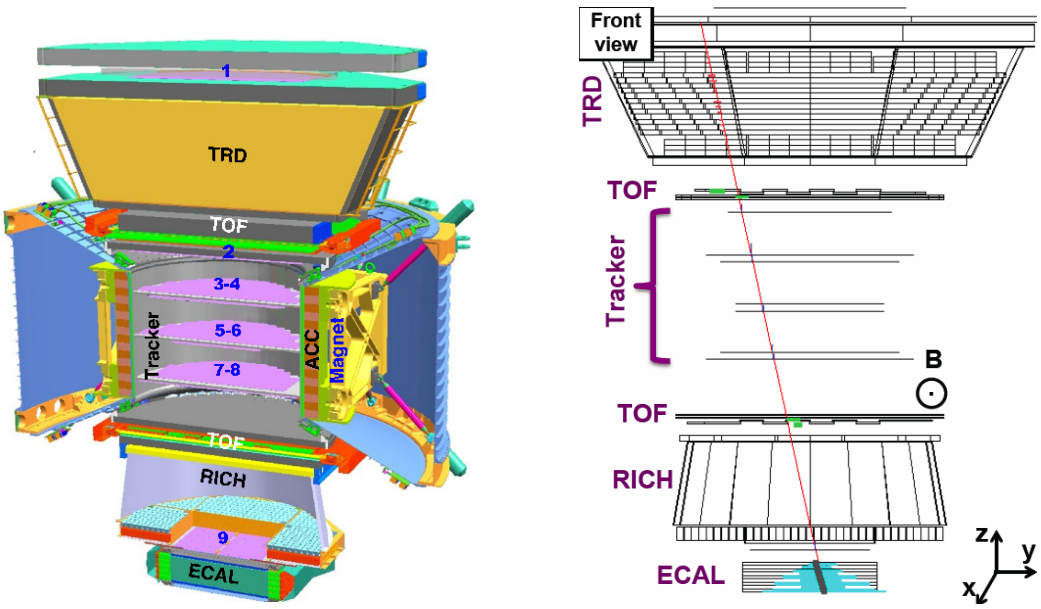

Figure 1: Left - Schematic view of the AMS-02 spectrometer. Right - A 660 GeV electron measured by the AMS detector on the ISS in the bending (y-z) plane. Silicon Tracker planes measure the particle charge and momentum, identifying the particle as a unitary charge (Z=1), negative charge particle. The TRD identifies the particle as an electron. The TOF measures the charge and ensures that the particle is downward-going. The ECAL, independently from TRD, identifies the particle as an electron and measures its energy.

and its negative charge sign are determined from the measured curvature and the unitary charge is independently assessed from the energy deposit released in the different silicon layers.

The TRD and ECAL detectors are the key detectors used to distinguish electrons/positrons from the large proton background. The TRD exploits the differences in the energy deposit released in its 20 layers of proportional tubes interleaved with fleece radiator by same momentum light (e) and heavier (p) particles. The observed signals in all TRD layers associated to the reconstructed particle are combined in a TRD Classifier based on the log-likelihood for the electron hypothesis (TRD-LLe) (see Fig.2), which is then used either to cut or to estimate the proton component in the sample. The 3D imaging capability of the ECAL detector is exploited to distinguish between hadrons and leptons through the analysis of the shower topologies. A statistical estimator ECAL-BDT (boosted decision tree algorithm [15]), has been deployed by means of the different characteristics between electromagnetic and hadronic showers.

3. The data analysis strategy

The analysis has been restricted to particles with energies above the geomagnetic cutoff [14]. The electron measurement is performed in ECAL energy bins. The binning is chosen according to the energy resolution and the available statistics such that migration of the signal events to neighbouring bins has a negligible contribution to the systematic errors above 2 GeV. In each energy bin the data are fitted, with a standard template-fit approach, using the reference spectra of the TRD

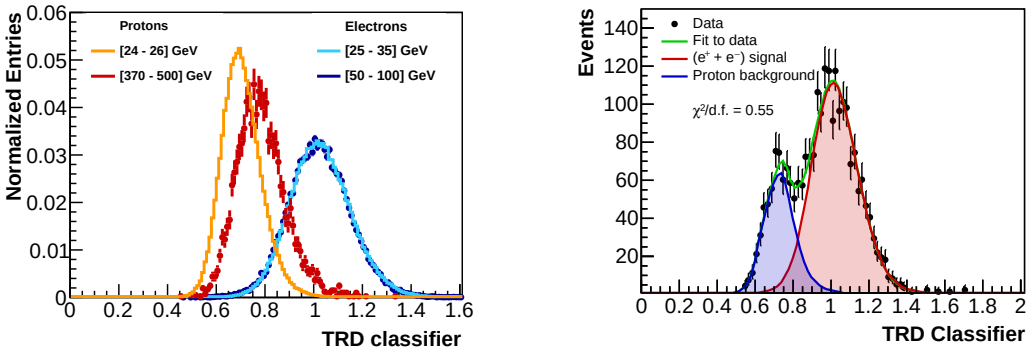

Figure 2: Left - TRD classifier distribution for electrons (blue and light blue) and protons (red and orange) in different energy ranges. The TRD-LLe, for electrons at energies greater than $\sim$ 10 GeV, does not dependent from the $e^{\pm}$ energy. Right - Signal and background components are fitted to determine the number of signal events. In the reported example (energy range 149-170 GeV) the $e^+ + e^-$ (protons) fitted reference spectrum is coloured in red (blue). The green line represents the overall fit superimposed on the black data points.

Classifier, to determine the numbers of signal (background) events in the total sample. The reference spectra for signal and background have been determined directly from the flight data: pure samples of electrons and protons have been selected by means of tight requirements on the ECAL shower shape, on the ratio between reconstructed momentum in the Tracker and measured energy in the ECAL (E/p), and on the reconstructed charge sign[1]. Fig.2 (left) shows the distribution of the TRD Classifier for electrons (blue and light blue) and protons (red and orange) in different energy ranges. The TRD Classifier reference spectrum for electrons does not depend on the $e^{\pm}$ energy and has been determined using the full statistics in the 15-80 GeV energy range, thus maximizing the used statistics at energies where the proton background can be efficiently removed. For the more abundant protons, the reference spectrum, which has a clear dependence on the energy, has been determined bin by bin from data. In Fig.2 (right) an example of the fitted signal and background distributions are presented at energies between 149 and 170 GeV.

4. The flux measurement

The electron flux in each energy interval [E,E+ΔE] is measured as :

$$\Phi(E) = \frac{N(E)}{A_{eff}(E)\ \varepsilon_{trig}(E)\ \varepsilon_{ECAL}(E)\ T(E)\ \Delta E}$$

where:

- N is the number of electron/positron events;
- T is the exposure time, 6.2×10^7 s at energies above 25 GeV, for 30 months of data taking;
- A_{eff} is the the effective detector acceptance, given by the geometrical acceptance, A_{geom}, after applying the event selection, with efficiency ε_{sel}, and corrected for all the residual discrepancies, δ, between data and MC. $A_{eff} = A_{geom}\ \varepsilon_{sel}\ (1+\delta)$;

[1] The positive (negative) sample is naturally enhanced in terms of protons (electrons)

- ε_{ECAL} is the efficiency of the signal selection based on the ECAL-BDT;
- ε_{trig} is the trigger efficiency;

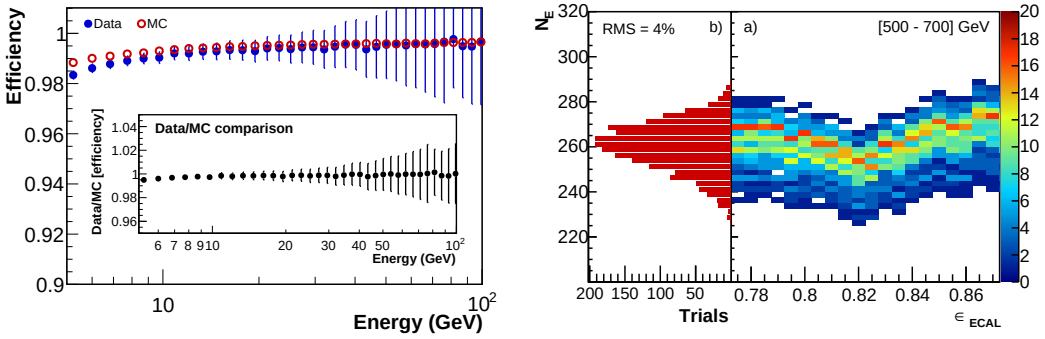

Figure 3: Left - TRD reconstruction efficiency as a function of energy for both ISS (full blue) and MC (open red) electrons. The ratio of the two curves, shown in the insert, is used to correct, if needed, the acceptance given by MC and to asses a systematic related to the correction itself. Right - Stability of the measured number of $e^+ + e^-$ as a function of the BDT cut efficiency (Fig. b). The spread (RMS) of the fitted number of $e^+ + e^-$, Fig. a, is used as systematics on the signal selection.

A full Geant4 [16] MonteCarlo (MC) simulation of the response of the AMS-02 detector to an isotropic electron spectrum has been developed to estimate the detector acceptance. The effect of each single selection has been compared between flight data and MC to validate the simulation and the obtained acceptance, A_{eff}. If needed, small corrections ($O(\%)$) have been applied to the acceptance obtained by MC. In Fig.3 left, for example, the TRD reconstruction efficiency is shown for both flight and MC electrons. The ratio between the two quantities (Fig.3 left, insert) is used to check the agreement between data and MC and to asses the systematic on the knowledge of the real acceptance.

To measure the trigger efficiency from data, a pre-scaled sample of events passing a looser trigger condition is also recorded as an *unbiased* sample. This allowed the determination of the trigger efficiency, ε_{trig} directly from the flight data. The ECAL-BDT efficiency, ε_{ECAL}, has been evaluated, also, directly from data, from a background free sample of electrons, selected with the negative charge sign. The template-fit analysis has been performed also on this sample at different BDT cuts. The ratio between fitted electrons at a given BDT cut with respect to the total number of fitted electrons in absence of ECAL selection defines the efficiency. The stability of the measurement against different choices of the BDT cut (e.g. different selection efficiencies) has been investigated in a wide range of calorimetric selection efficiencies (see Fig.3-right).

5. Results and Conclusions

The measurement of the electron spectrum with the AMS-02 detector has been performed at energies between 0.5 and 700 GeV and is reported in Fig.4 (top-right). The measurement of the positron spectrum has been performed up to 500 GeV, Fig.4 (top-left) and the $e^+ + e^-$ flux has been performed up to 1 TeV, Fig.5 (left). The separate positron and electron fluxes have been

measured using the same analysis and distinguishing the two species by means of the charge sign measured in the Silicon Tracker. Conceptually the $e^+ + e^-$ flux could be computed by summing the two separate fluxes: a detailed and distinct analysis has been instead developed. This allowed to reach high energies in the flux measurement with a reduced systematics uncertainty. In the $e^+ + e^-$ measurement, indeed, there was no need to explicitly distinguish the $e^\pm$ by their charge sign: no selection cuts were therefore applied on the quality of the tracking to minimize charge confusion effects. This lead to a larger statistics of the selected sample and avoided the systematic uncertainties related to the finite knowledge of the track selection efficiencies.

No evidence of structures has been found in the 3 energy spectra. The raise in the positron flux, at energies greater than ~ 30 GeV clearly indicates how the raise in the positron fraction must be attributed to an hardening of the positron spectrum rather than a lack of high energy electrons. In particular the feature observed by ATIC and PPB-BETS [5] in the $e^+ + e^-$ spectrum has not been confirmed. In the published papers [4, 3] a detailed study of the spectral indices as function of energy allow an accurate and unprecedented understanding of the observed spectral behaviours. For example, as shown in Fig.5 (right), above ~ 30 GeV the flux can be described by a single power law with spectral index $\gamma = -3.170 \pm 0.008\,(\text{stat + syst}) \pm 0.008\,(\text{energy scale})$.

For these measurements, ~ 10 million electrons/positrons have been selected from more than 41 billion triggers collected in 30 months of operations in space. This represents $\sim 10\%$ of the final expected data sample for the whole AMS mission duration.

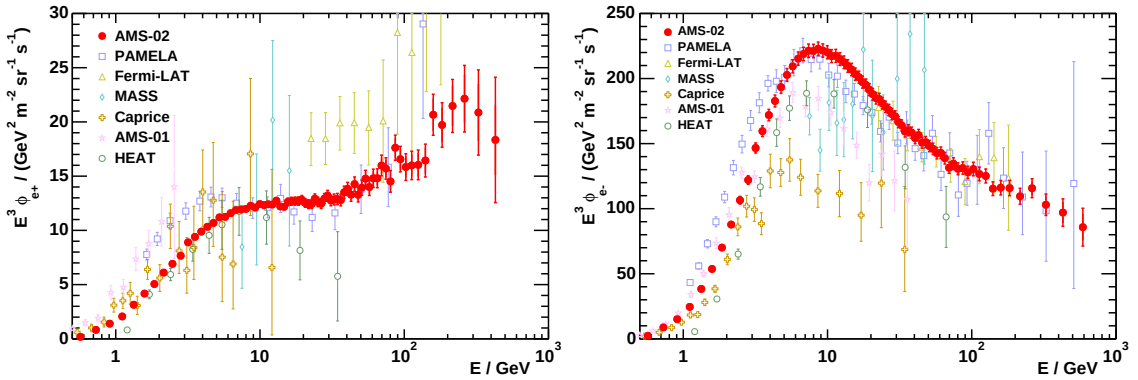

Figure 4: Left - AMS positron flux (red points) as a function of the energy, superimposed to the most recent measurements by other experiments. Right - AMS electron flux (red points) as a function of the energy, superimposed to the most recent measurements by other experiments.

Acknowledgments

This work has been supported by acknowledged persons and institutions in the published papers about the AMS-02 electron and positron measurements [2, 3, 4], as well as by the Italian Space Agency under contracts ASI-INFN I/002/13/0 and I/037/14/0.

References

[1] M. Aguilar *et al. Phys. Rev. Lett.* **110**, 141102 (2013)

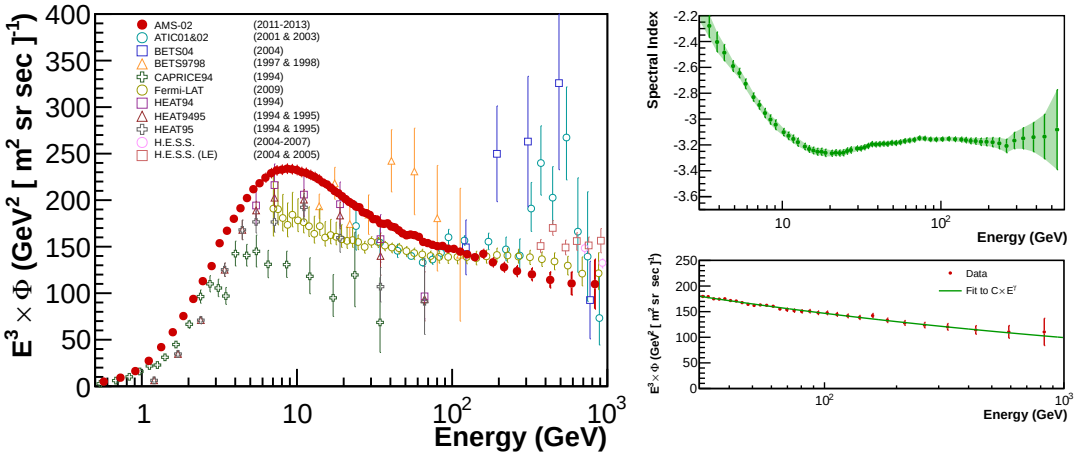

Figure 5: Left - AMS combined electron plus positron spectrum (red points) as a function of the energy, superimposed to recent measurements from other experiments. Right top - Spectral index of the combined electron plus positron spectrum as a function of the energy. Right bottom - High energy part of the combined electron plus positron flux fitted with a single power law.

[2] L. Accardo *et al.* *Phys. Rev. Lett.* **113**, 121101 (2014)

[3] M. Aguilar *et al.* *Phys. Rev. Lett.* **113**, 121102 (2014)

[4] M. Aguilar *et al.* *Phys. Rev. Lett.* **113**, 221102 (2014)

[5] J. Chang *et al* *Nature* **456**, 362 -365 (2008)

[6] S. Torii *et al* ArXiv:0809.0760

[7] M. Ackerman *et al* *Phys. Rev. D* **82**, 092004 (2010)

[8] M. Ackerman *et al* *Phys. Rev. Lett.* **108**, 011103 (2012)

[9] O. Adriani *et al.* *Nature* **458**, 607-609 (2009).

[10] P. Blasi *Phys. Rev. Lett.* **103**, 051104 (2010)

[11] L. Feng *et al.* *Physics Letters B* **728**, 250 - 255 (2014)

[12] L. Bergström *et al.* *Phys. Rev. Lett.* **111**, 171101 (2013)

[13] I. Cholis *et al.* *Phys. Rev. D* **88**, 023013 (2013)

[14] C. Störmer *Q.J.R. Meteorol. Soc* **82**, 115 (1956).

[15] B. P. Roe *et al.* *Nucl. Instrum. Methods Phys. Res., Sect. A* **543**, 2-3 (2005)

[16] S. Agostinelli *et al.* *Nucl. Instrum. Methods Phys. Res., Sect. A* **506**, 250 (2003)

[17] F. Aharonian *et al* *Phys. Rev. Lett.* **101**, 261104 (2008),*A&A* **508**, 561-564 (2009)

[18] F. Aharonian *et al* *A&A* **508**, 561-564 (2009)

[19] T. Delahaye *et al* *Astron. & Astroph.* **524**, A51 (2010)

[20] O. Adriani *et al* *Phys. Rev. Lett.* **106**, 201101 (2011)